

# High-efficiency photovoltaic devices based on annealed poly(3-hexylthiophene) and 1-(3-methoxycarbonyl)-propyl-1-phenyl-(6,6) $C_{61}$ blends

Marisol Reyes-Reyes, Kyungkun Kim, and David L. Carroll<sup>a)</sup>

*The Center for Nanotechnology and Molecular Materials, Department of Physics, Wake Forest University, Winston-Salem, North Carolina 27109*

(Received 11 March 2005; accepted 27 June 2005; published online 18 August 2005)

The effects of annealing and fullerene loading in regioregular poly(3-hexylthiophene) (P3HT) and 1-(3-methoxycarbonyl)-propyl-1-phenyl-(6,6) $C_{61}$  (PCBM) based bulk heterojunction photovoltaics have been investigated. Under specific loading and annealing conditions, a combination of morphological and electronic factors can be brought to play to achieve optimal filling factors, open-circuit voltage ( $V_{oc}$ ), and short-circuit current density ( $J_{sc}$ ). We demonstrate that this occurs at surprisingly low loadings of PCBM and annealing temperatures nearing the melting point of the polymer. Further, we report power conversion efficiencies approaching 5% in the P3HT:PCBM system. © 2005 American Institute of Physics. [DOI: 10.1063/1.2006986]

The use of organic conjugated polymers as a photovoltaic system has seen an exciting growth in interest recently as developments in organic synthesis and device fabrication technologies have continued to raise the power conversion efficiencies. Perhaps one of the most exciting systems is based on the poly(3-alkylthiophene) family of polymers. Specifically, photovoltaic power conversion efficiencies of 1.5% and 3.5% have been reported now by research groups working with poly(3-octylthiophene) (Ref. 1) and P3HT,<sup>2</sup> respectively. The most common approach, and indeed the approach to the highest efficiencies in this system are based on bulk heterojunction formation within the photoactive layer using PCBM, a fullerene derivative, as an electron acceptor nanophase. Conceptually, this phase allows for bulk separation of photoinduced excitons, and high mobility removal of the “electron” through the nanophase. The thiophene host phase typically has high “hole” mobilities<sup>3</sup> and thus the devices remain charge balanced allowing for relatively large filling factors to be generated.

The difficulty in these systems arises when we account for the effects of morphological modifications in the thiophene phase due to the introduction of the nanophase. That is, properties of the thiophene host phase: Crystallization, mobility, etc., might well depend on the properties of the blended nanophase, yielding unsuspected consequences to the performance of the device. Thus, there have been a significant number of studies that investigate the effects of processing parameters in the blended photoactive phase. Unfortunately, no conclusive result as to the optimal processing of the nanophase for device performance has been obtained to date. In fact, the most recently high efficiency cells were reported with concentrations of the nanophase PCBM as 1:4 with the poly[2-methoxy-5-(3',7'-dimethyloctyloxy)-1,4-phenylene vinylene] (MDMO-PPV) (Ref. 4) whereas with P3HT ratios between 1:2 and 1:3 have been studied.<sup>2,5</sup> In the case of polythiophene and PCBM the optimum weight ratio is still unclear. However, Chirvase *et al.*<sup>6</sup> show that the maximum power conversion efficiency occurs between 1:1 and

1:0.9. Further, the charge balance depends on overall film thickness and most researchers do not disclose under which conditions their optimal concentrations are relevant.

In this work, we examine directly the effects annealing in an “optimally filled” PCBM:P3HT organic photovoltaic device at a specific film thickness. In this study, optimal loading values were determined for unannealed devices and the effects of post fabrication annealing yield power conversion efficiencies that approach 5%.

Thin film photovoltaic devices were prepared by first dissolving the PCBM (American Dye Source) in chlorobenzene. P3HT (Aldrich: Regioregular with an average molecular weight,  $M_w=87$  kg mol<sup>-1</sup>, without further purification) was blended into the PCBM solutions. Subsequently, the blend was filtered (0.2  $\mu$ m, Teflon).

The devices were prepared on glass/indium-tin oxide (ITO) (delta technologies  $R_s=10$  Ohm square<sup>-1</sup>) substrates. The substrates were thoroughly cleaned in an ultrasonic bath with methanol, acetone, and isopropyl alcohol successively for 20 min, and dried in a dry nitrogen stream. The substrates were then exposed to ozone for 90 min. Poly(3,4-ethylenedioxythiophene):poly(styrenesulfonate) (PEDOT:PSS) (Baytron P) was deposited by spin coating at 4000 rpm and then dried at 80 °C for 10 min. Subsequently, the P3HT:PCBM solutions were deposited through spin casting at 1500 rpm. The morphology of representative films was determined using atomic force microscopy [(AFM) JEOL JSPM-5200] in noncontact mode (because these were exposed to atmospheric conditions for long times during imaging, they were not used for the creation of test devices). LiF (Aldrich) and Al (Sigma-Aldrich) electrodes were deposited via thermal evaporation with approximately 3–4 Å and 100 nm thick, respectively. The active layer is 0.19 cm<sup>2</sup>. Once the electrodes were deposited, the devices were encapsulated in an inert atmosphere (dry nitrogen glovebox).

It is known that in polymer: Fullerene bulk heterojunctions the open-circuit voltage ( $V_{oc}$ ) is derived primarily by the energy difference between the lowest unoccupied molecular orbital of the acceptor and the highest occupied molecular orbital of the donor. However, the dependence on fullerene content in the bulk heterojunction has also been

<sup>a)</sup> Author to whom correspondence should be addressed; electronic mail: carrolldl@wfu.edu

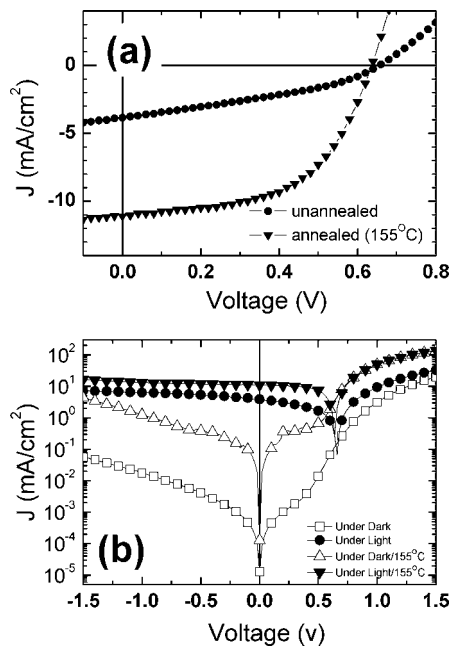


FIG. 1.  $J$ - $V$  characteristics of ITO/PEDOT:PSS/P3HT:PCBM/LiF/Al heterojunction unannealed and annealed device (a) in a linear plot and (b) in a logarithmic scale.

observed to affect the  $V_{oc}$ , short-circuit current density ( $J_{sc}$ ), and efficiency values ( $\eta$ ).<sup>6,7</sup> The optimal ratio of PCBM to P3HT, for these studies, was determined from unannealed devices separately. The ratio was varied such that the solution's solid content was a constant, yielding a constant film thickness for the active layer in each device at a given spin speed. In the unannealed devices, an optimal PCBM:P3HT ratio of 0.8:1 was found in rough agreement with other sources.<sup>6</sup> For the unannealed devices, the performance characteristics were:  $V_{oc}=0.65$  V,  $J_{sc}=3.86$  mA cm<sup>-2</sup>, FF (fill factor)=0.34, and  $\eta_{pc}$  (power conversion efficiency) =1.11%. We note that these values are in slight variation with those found by other researchers. However, the device structures used in those studies are slightly different.

Once the optimal loading was determined for the active layer, and holding all other variables constant, a set of three devices were fabricated using the 0.8:1 PCBM:P3HT loading ratio, encapsulated (as described above) and then annealed at 80 °C, 105 °C, and 155 °C for different times in the study. We note that the melting point temperature of P3HT (regio-regular) has been reported to be  $\sim 230$  °C by differential scanning calorimetry analysis.<sup>8</sup>

All device measurements were performed at room temperature. The current-voltage ( $I$ - $V$ ) curves of the devices were measured using a Keithley 236 Source Measure Unit. The solar simulator used was an AM1.5G from Oriol. The illumination intensity used was 80 mW cm<sup>-2</sup>. The intensity in the simulator was adjusted with neutral density filters and calibrated with a National Institute of Standards photodetector.

Shown in Fig. 1 is a comparison of the  $I$ - $V$  response (curves) from annealed and unannealed devices. The unilluminated  $I$ - $V$  characteristics or "dark conditions  $I$ - $V$ s" are shown as squares in Fig. 1(a) for the unannealed devices and triangles in Fig. 1(a) for devices annealed at 155 °C for 5 min. The overall shape of the curves under dark, forward bias conditions is essentially the same suggesting that little

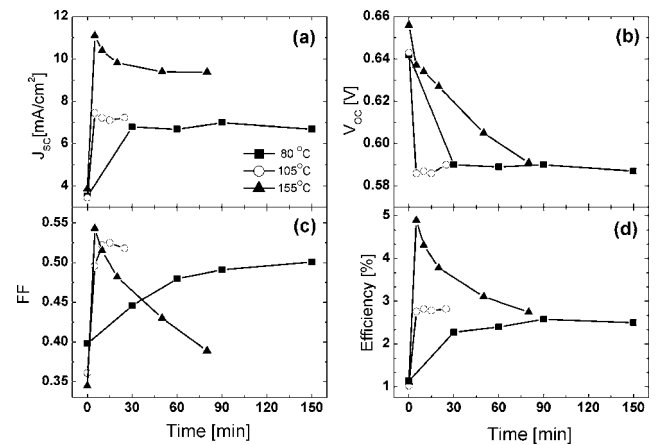


FIG. 2. Influence of the duration of the annealing on (a) the short-circuit current density, (b) open-circuit voltage, (c) FF, and (d) power conversion efficiency for different temperatures.

modification to band bending at the interfaces has occurred due to heating. In the dark, under reverse bias, no changes in the  $I$ - $V$  slope have occurred. However, a substantial offset in the current is observed reflecting the higher overall mobility. The illuminated curves also show this offset with few other differences.

Shown in Fig. 2 are the performance characteristics as each of the devices are annealed. We note that since the devices are encapsulated, they generally show constant performance characteristics over the time frames of the experiments presented here. Each of the curves was collected for a single device, i.e., triangle in Fig. 2 is one device annealed and tested then annealed for longer periods and tested consequently, etc. Notice that for the highest-temperature device, the performance (as determined by power conversion efficiency), and FF decreases with annealing time [shown in triangle in Figs. 2(d) and 2(c), respectively]. However, for both of the lower-temperature annealed devices, the performance continues to rise with annealing time. This suggests a thermally activated kinetic process for the improvement in device performance. We suggest that this is not due to the removal of solvent but rather, better polymer chain ordering within the thin film allowing for high mobilities (as reflected in the FF curve). While the electronic transport mechanism in P3HT is not rigorously established, due to its complex heterogeneous structure on a mesoscopic length scale, structural order and orientation influences on the electronic properties have been observed (cf., e.g., Siringhaus *et al.*).<sup>9</sup> It has been reported that when a polythiophene is annealed to a temperature higher than its glass-transition temperature, enhanced crystallization of the polymer results.<sup>10</sup> As a result of this crystallization, hole conductivity of the polythiophene increases dramatically.<sup>11,12</sup>

The temperature dependence of the short-circuit current has been previously observed in polymer-fullerene,<sup>13,14</sup> polymer-PBCM (Ref. 15) photovoltaic devices. In our case, the maximum  $J_{sc}$  occurred at 155 °C for 5 min annealing times [Fig. 2(a)]. The maximum  $J_{sc}$  obtained was reached (11.1 mA cm<sup>-2</sup>), larger than those seen in previous reports. The large  $J_{sc}$  value is surprising since the PCBM nanophase, in our case, is so diffuse that fullerene-fullerene hopping should be relatively small at room temperature. However, the overall polymer crystallinity has improved due to annealing as stated above. Thus, hole mobility has likely increased. We

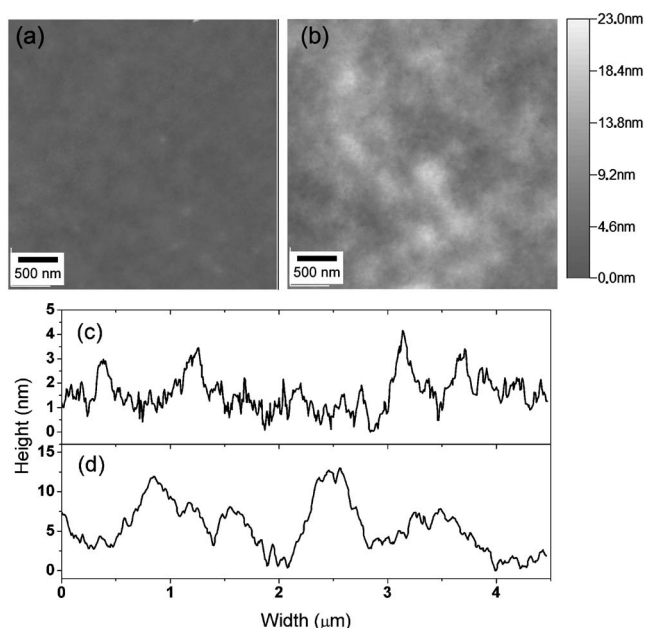


FIG. 3. AFM comparison of P3HT:PCBM, and their respective profile analysis [(a) and (c)], unannealed and [(b) and (d)] annealed (155 °C, 5 min) composite films.

note that our devices show an increase in FF from 0.34 to 0.54, as we increase the annealing temperature from 80 °C to 155 °C [Fig. 2(c)]. This suggests an increase in carrier transport and results in an overall power efficiency of  $\eta_{pc} \sim 4.9 \pm 0.2\%$  [Fig. 2(d)].

The sharp change in performance parameters, such as  $V_{oc}$ , and  $J_{sc}$ , cannot be explained fully by changes in the overall polymer crystallinity for bulk heterojunction systems. It has been observed by other researchers that  $V_{oc}$  can depend strongly on the PCBM loading levels.<sup>7</sup> Two competing views of this phenomenon have been taken. The first is that this is purely an electronic effect, and arises due to the overall change in itinerate carrier concentration. This, correspondingly, yields changes in the band bending at the electrodes. Alternatively, it has been suggested that the morphology of the PCBM nanophase changes with loading, leaving more aggregate clusters near the contacts of the device at higher loadings.<sup>7</sup> In these studies, the loading levels were held constant and the overall film morphology was modified through annealing. This leads to the same observed trends as for the increase in loading. That is, as the films are annealed the  $V_{oc}$  decreases as shown in Fig. 2(b). This behavior was also observed by Chirvase *et al.*<sup>15</sup> We interpret this as resulting from diffusion of the PCBM phase away from the contact area. This is supported by the changes observed in the overall film morphology as determined by AFM. Shown in Fig. 3 are images of film before and after annealing. Notice in the before case [Fig. 3(a)] and [Fig. 3(c)], the film is rough over very fine ( $<0.1 \mu\text{m}$ ) length scales. After annealing, the root-mean-square (rms) height variation increases over the micron scale, but at the submicron level, the film is relatively

smooth. We attribute the smaller features seen in the unannealed films to very small aggregates of PCBM, whereas in the annealed film, feature size is significantly larger, suggesting larger aggregates, perhaps covered by a polymer layer, are present. While this is clearly not conclusive, it does support the view that aggregate morphology is the likely explanation for shifts in the  $V_{oc}$  both in our studies (with annealing) and with loading as observed by other researchers.

In summary, we have presented the effects of annealing in a PCBM:P3HT photovoltaic device. The studies were done with a single loading ratio of PCBM to P3HT, found to be optimum in the unannealed system. Short-time annealing treatments of 155 °C were found to result in devices that have a conversion efficiency of  $\sim 4.9\%$ ,  $V_{oc}=0.6$  V, and  $J_{sc}$  of  $11.1 \text{ mA cm}^{-2}$ . Moreover, analysis of changes in the film morphology suggests that these improved photovoltaic characteristics arise due to changes in the films crystallinity and aggregation within the films PCBM nanophase. This leads to the natural conclusion that such morphological control over bulk heterojunction systems might provide a route to higher efficiency organic devices in the future.

One of the authors (M.R.R.) thanks Dr. R. López-Sandoval for many fruitful discussions. This work was supported at Wake Forest University by the Air Force Office of Sponsored Research (AFOSR) under Grant No. FA9550-04-1-0161.

- <sup>1</sup>D. Gebeyehu, C. J. Brabec, F. Padinger, T. Fromherz, J. C. Hummelen, D. Badt, H. Schinler, and N. S. Sariciftci, *Synth. Met.* **118**, 1 (2001).
- <sup>2</sup>F. Padinger, R. S. Rittberger, and N. S. Sariciftci, *Adv. Funct. Mater.* **13**, 85 (2003).
- <sup>3</sup>S. S. Pandey, W. Takashima, S. Nagamatsu, T. Endo, M. Rikukawa, and K. Kaneto, *Jpn. J. Appl. Phys., Part 1* **39**, 94 (2000).
- <sup>4</sup>S. E. Shaheen, C. J. Brabec, S. Sariciftci, F. Padinger, T. Fromherz, and J. C. Hummelen, *Appl. Phys. Lett.* **78**, 841 (2001).
- <sup>5</sup>P. Schilinsky, C. Waldauf, and C. J. Brabec, *Appl. Phys. Lett.* **81**, 3885 (2002).
- <sup>6</sup>D. Chirvase, J. Parisi, J. C. Hummelen, and V. Dyakonov, *Nanotechnology* **15**, 1317 (2004).
- <sup>7</sup>J. K. J. van Duren, X. Yang, J. Loos, C. W. T. Bulle-Lieuwma, A. B. Sieval, J. C. Hummelen, and R. A. J. Janssen, *Adv. Funct. Mater.* **14**, 425 (2004).
- <sup>8</sup>S. Hugger, R. Thomann, T. Heinzl, and T. Thurn-Albrecht, *Colloid Polym. Sci.* **282**, 932 (2004).
- <sup>9</sup>H. Sirringhaus, P. J. Brown, R. H. Friend, M. M. Nielsen, K. Bechgaard, B. M. W. Langeveld-Voss, A. J. H. Spiering, R. A. J. Janssen, E. W. Meijer, P. Herwig, and D. M. de Leeuw, *Nature (London)* **401**, 685 (1999).
- <sup>10</sup>Y. Zhao, G. X. Yuan, P. Roche, and M. Leclerc, *Polymer* **36**, 2211 (1995).
- <sup>11</sup>J. J. Dittmer, E. A. Marsiglia, and R. H. Friend, *Adv. Mater. (Weinheim, Ger.)* **12**, 1270 (2000).
- <sup>12</sup>M. Nakazono, T. Kawai, and K. Yoshino, *Chem. Mater.* **6**, 864 (1994).
- <sup>13</sup>E. A. Katz, D. Faiman, S. M. Tuladhar, J. M. Kroon, M. M. Wienk, T. Fromherz, F. Padinger, C. J. Brabec, and N. S. Sariciftci, *J. Appl. Phys.* **90**, 5343 (2001).
- <sup>14</sup>I. Riedel, J. Parisi, V. Dyakonov, L. Lutsen, D. Vanderzande, and J. C. Hummelen, *Adv. Funct. Mater.* **14**, 38 (2004).
- <sup>15</sup>D. Chirvase, Z. Chiguvare, M. Knipper, J. Parisi, V. Dyakonov, and J. C. Hummelen, *J. Appl. Phys.* **93**, 3376 (2003).